

## 2002年度日中医学協会共同研究等助成事業報告書

—在留中国人研究者研究助成—

2003 年 3 月 5 日

財団法人 日中医学協会  
理事長 殿

研究者氏名 郭 麗梅 

所属機関名 高知医科大学第一病理学教室

指導責任者氏名 円山 英昭

職 名 教授

所 在 地 〒83-8505 高知県南国市岡豊町小蓮 210 番地

電話 088-880-2332 内線 2632

### 1. 研究テーマ

肝線維化の病理学的及び分子生物学的研究

### 2. 本年度の研究業績

(1) 学会・研究会等における発表  有 ・  無 (学会名・演題)

1. 第三回細胞病理談話会 (2002. 8. 3-4、熊本大学医学部):

Distribution and function of vinculin in human hepatic stellate cell

2. 第二回 Kochi Medical School Research Meeting (2003. 2. 20-21. 高知医大)

Cellular aspects of iron-induced rat liver fibrosis

(2) 学会誌等に発表した論文 有 ・  無 (雑誌名・論文名)

## Dimethylnitrosamine (DMN) 1回大量投与ラットの 肝線維化モデルにおける鉄の過剰沈着と線維化との相関

研究者氏名 郭 麗梅  
中国所属機関 中国哈爾濱医科大学第二附属医院 病理部  
日本研究機関 高知医科大学第一病理学教室  
指導責任者 教授 円山 英昭  
共同研究者名 金 玉蘭、戸井 慎、黒田 直人、弘井 誠、林 芳弘、宮崎 恵利子

### Abstract

In this study, we investigated the cellular basis of iron-associated rat liver fibrosis induced by a high dose injection of dimethylnitrosamine (DMN). Histologically, liver injury reached a peak at 36h after the injection and showed a submassive hemorrhagic necrosis. On day 3, hepatic stellate cells (HSCs) positive for  $\alpha$ -smooth muscle actin (ASMA) appeared in preserved parenchyma. With time, necrotic tissues and erythrocytes were phagocytosed by macrophages and on day 5, a large amount of macrophages containing iron were observed in the necrotic areas. ASMA-positive HSCs distributed along the margin between necrotic areas and residual remaining liver parenchyma. On day 7, activated HSCs were diffusely distributed along the sinusoids and thin fibrous septa. On day 14, central-to-central bridging fibrosis was formed. In the fibrous septa, macrophages containing iron were in close proximity to the collagen-producing myofibroblasts. Afterthat, the extent of fibrosis increased in parallel with the infiltration intensity of iron-containing macrophages. To our interest, even on months 1, 3, and 6 after injection, a striking iron deposition in macrophages in the fibrous septa was sustained. Among the cytokines released in liver diseases, TNF- $\alpha$  plays a crucial role in liver inflammation and hepatic regeneration. In our study, immunohistochemically, TNF- $\alpha$ -positive macrophages were observed focally at 12h after injection, and they increased in the necrotic areas at days 5 and in the thin fibrous septa at week 1. Moreover, a few TNF- $\alpha$ -positive macrophages were observed at week 2 and month 1. RT-PCR analysis showed positivity at 12h, 3d, 1w after the injection. These results confirmed the roles of TNF- $\alpha$  in liver fibrosis. However, whether TNF- $\alpha$  may be directly involved in rat liver fibrosis and the association between iron deposition and TNF- $\alpha$  expression needs to be studied further. In brief, we provides a potential model for the study of iron-induced liver fibrosis and the association between macrophages and HSCs. Iron deposition may be dramatically involved in the development and sustenance of liver fibrosis. Furthermore, the iron-containing macrophages may influence HSCs through the action of cytokines and play a significant role in the DMN-induced liver fibrosis.

**Key Words** iron deposition, liver fibrosis, hepatic stellate cells, macrophages

### Introduction:

Previous studies have suggested that excess hepatic iron accumulation is a progressive factor in some liver diseases

including chronic viral hepatitis, hemochromatosis, liver cirrhosis and liver cancer (1-4). However, it has not been clarified whether iron-induced hepatotoxicity is directly involved in liver fibrosis. Previous *in vivo* experimental models provided that iron overload may enhance the accumulation of hepatic collagen I mRNA in rodents, especially in hepatic stellate cells (HSCs) (5). The cellular iron toxicity is proposed to be mainly due to iron-induced free radical attack and iron-induced lipid peroxidation damage (6,7). On the other hand, during the liver injury, several cytokines and growth factors, including IL-1, IL-6, IL-8, IFN- $\gamma$ , TGF- $\beta$ , PDGF, and TNF- $\alpha$  were reported to be increased (8-14). Among them, TNF- $\alpha$  has pleotropic functions on proinflammation, cell proliferation and apoptosis, but its role in liver fibrosis has not yet been confirmed. Therefore, in this study we investigated the cellular aspects of iron-induced rat liver fibrosis and whether iron may contribute to the development and progression of liver fibrosis, and the role of TNF- $\alpha$  in this process.

### **Materials and Methods:**

*Animals and tissues* Male Wistar rats (200-250g) were used for DMN-induced liver injuries. Additionally, three untreated rats and three saline-injected rats were used as normal controls. Hepatic injury was induced by an intraperitoneal injection of DMN (WaKo) 50mg/Kg of body weight. To study the morphological changes of liver, three rats per each group were sacrificed at 6, 12, 24, 36 hours and 2, 3, 5, 7, 10, 14 days and 1, 2, 3, 6, and 10 months after the injection. Portions of liver tissue from control and treated rats were fixed in 10% formalin for histological processing and in 4% paraformamide for *in situ* hybridization, and the remaining tissues stored at -80°C for RT-PCR analysis.

*Histological assessment* HE stain for morphologic evaluation and Berlin blue stain for assessment of iron load were performed. Evaluation of the staining intensity is graded as -, negative; +, mild; ++, moderate; +++, high expression.

*Immunohistochemistry* Immunohistochemical staining was carried out by using streptavidin-biotin peroxidase (SAB) method. Monoclonal antibodies for  $\alpha$ -smooth muscle actin (1A4, DAKO, 1:50), ED-1 (Serotec, 1:500), and polyclonal antibody for TNF- $\alpha$  (Endogen, 1:50) were used.

*In situ hybridization* Rat  $\alpha 2$  (I) collagen RNA probes for *in situ* hybridization were created by using specific primers (Forward: 5' AACAGGACTTCTTCGGAACCAC3'; Reverse: 5' CATTTCGACCACTTGTGGCTTC3') and RT-PCR amplification of a 422bp fragment. PCR product was purified and ligated to pGEM-T easy (Promega) according to the protocol. Then it was transformed and extracted using Midiprep kit (Qiagen). The sequence was linearized by digestion of NheI or SphI. Sense and antisense collagen I probes was labeled with digoxin by *in vitro* transcription assay (Roche). 4% paraformamide-fixed paraffin-embedded sections were used for *in situ* hybridization analysis as previously indicated.

*RT-PCR* RNA was extracted from frozen liver tissues by using RNeasy Mini Kit (Qiagen) according to the manufactures instructions. Rat  $\beta$ -actin and TNF- $\alpha$  primer sets (MBI) were used for PCR analysis.

### **Results:**

The morphological changes observed in a high-dose DMN-treated rats have been extensively reported in our previous studies (15). Briefly, normal rat livers (Fig.1) were injured after the injection and reached a peak at 36h, showing a submassive hemorrhagic necrosis (Fig.2). On day 3, HSCs positive for ASMA appeared in the preserved parenchyma. With time, necrotic tissues and erythrocytes were phagocytosed by macrophages. On day 5, ASMA-positive HSCs were distributed along the margin between necrotic areas and residual remaining liver parenchyma and a large number of macrophages containing iron occurred in the necrotic areas (Fig.3). On day 7, first sign of fibrosis was shown (Fig.4), and HSCs (myofibroblasts) and macrophages were diffusely distributed along the sinusoids and thin fibrous septa. On

day 14, central-to-central bridging fibrosis was formed throughout liver lobes (Fig.5). In the fibrous septa, macrophages laden with iron were in close proximity to the collagen-producing myofibroblasts (Fig.6). Afterthat, the extent of fibrosis increased in parallel with the infiltration intensity of iron-containing macrophages. Even on months 1, 3, 6, and 10, a striking iron deposition in macrophages in the fibrous septa was sustained (Fig.7). Immunohistochemically, ASMA-positive HSCs and ED-1-positive macrophages were shown on day 7 (Fig.8,9). On hours 12, 24, 36 and days 2, 3, TNF- $\alpha$ -positive macrophages were mildly appeared in the necrotic areas. A rapid increase was observed on day 4 and it kept the tendency until day 10 (Fig.10). Using antisense probe, in situ hybridization of collagen ( $\alpha$ 2) I confirmed the presence of activated HSCs on week 2. The signals were clearly observed in the cytoplasm of the activated HSCs in the fibrous septa (Fig.11). In keep with these observations, ultrastructural examination of livers at day 10 showed numerous macrophages laden with iron, activated HSCs, and the presence of transitional cells between HSCs and myofibroblasts (Fig.12). Using RT-PCR analysis, we detected a weak content of TNF- $\alpha$  on hours 12, 24, 36, day 3, and week 1. Chronological summary of liver injuries, iron deposition and immunohistochemical staining intensity was shown in Table 1.

### **Discussion:**

Previous in vivo experimental models made by long time feeding with iron-dextran showed two patterns of iron deposition in the livers (16, 17). Namely, iron was mainly present in the parenchymal cell resembling in hemochromatosis or in nonparenchymal cell foci, as secondary iron overload states. But the association of liver fibrosis with iron deposition has not yet been reported. Herein, liver fibrosis induced by a high dose injection of DMN may be a potential animal model for the study of iron-induced fibrosis.

Response to the sudden submassive necrosis and hemorrhage, monocytes originated from the bone marrow may dramatically influxed to necrotic and hemorrhagic areas, forming a phagocytosing macrophages stream. On the other hand, some experimental evidences have suggested that cytokines secreted by activated Kupffer cells and factors released by hepatocytes undergoing oxidant stress are responsible for the transformation of quiescent HSCs migrated into the necrotic areas from day 5 after the injection, and afterthat, both of them existed in the fibrous septa even in 10 months after injection. Such findings may suggest activated macrophages containing iron are responsible for recruitment of a large number of activated HSCs and for enhanced transcripts of collagen genes.

Among the cytokines released in liver diseases, TNF- $\alpha$  plays a crucial role in inflammation and hepatic regeneration (12). In our study, TNF- $\alpha$ -positive macrophages were observed focally at 12h after injection. They increased in the necrotic areas at days 5 and in the fibrous septa at week 1. These results confirmed the roles of TNF- $\alpha$  in liver fibrosis. However, whether TNF- $\alpha$  may be directly involved in rat liver fibrosis and the association between iron deposition and TNF- $\alpha$  expression needs to be studied further.

Herein, we provide a potential model for the study of iron-induced liver fibrosis and the interactions between macrophages and HSCs. In conclusion, iron deposition may be dramatically involved the development and progression of liver fibrosis. Furthermore, the iron-containing macrophages may influence HSCs through the action of cytokines and play a significant role in the DMN-induced liver fibrosis.

### **References:**

1. Di Bisceglie, A.M. et al., Measurement of iron status in patients with chronic hepatitis. *Gastroenterol* 1992, 102:2108-2113

2. Bassett, M. L. et al., Value of hepatic iron measurement in early hemochromatosis and determination of the critical iron level associated with fibrosis. *Hepatology* 1986, 6:24-29
3. Andorno, R.S. et al., et al., Iron, hepatic stellate cells and fibrosis in chronic hepatitis C. *Eur J Clin Invest* 2002, 32:28-35
4. Kato J. et al., Hepatic iron deprivation prevents spontaneous development of fulminant hepatitis and liver cancer in Long-Evans Cinnamon rats. *J Clin Invest* 1996, 98: 923-929
5. Pietrangelo, A. et al., Enhanced hepatic collagen I mRNA expression into fat-storing cells in a rodent model of hemochromatosis. *Hepatology* 1994, 19:714-721
6. Khan, F.M. et al, Protein adducts of malondialdehyde and 4-hydroxynonenal in livers of iron loaded rats: quantitation and localization. *Toxicol* 2002, 173:193-201
7. Baroni G.S. et al., Fibrogenic effect of oxidative stress on rat hepatic stellate cells. *Hepatology* 1998, 27:720-726
8. Macdonald G.A. et al., Lipid peroxidation in hepatic steatosis in humans is associated with hepatic fibrosis and occurs predominately in acinar zone 3. *J Gastroenterol and Hepatol* 2001, 16:599-606
9. Zylberberg H. et al., Soluble tumor necrosis factor receptors in chronic hepatitis C: a correlation with histological fibrosis and activity. *J Hepatol* 1999, 30:185-191
10. Jacquelyn J.M. et al., Interactions between hepatic stellate cells and the immune system. *Semi Liver Disease* 2001, 21:4117-426
11. Pietragelo A. et al., Metals, oxidative stress, and hepatic fibrogenesis. *Semi Liver Disease* 1996, 16:13-30
12. Pinzani M. et al., Cytokine and signaling in hepatic stellate cells. *Semi Liver Disease* 2001, 21:397-416
13. Kitamura L. et al., Pathogenic roles of tumor necrosis factor receptor p55-mediated signals in dimethylnitrosamine-induced murine liver fibrosis. *Lab Invest* 2002, 82:571-583
14. Tilg H. et al., Cytokines receptors and liver diseases, *Can J Gastroenterol* 2001, 15:661-668
15. Jin Y.L. et al., Tissue remodeling following submassive hemorrhagic necrosis in rat livers induced by an intraperitoneal injection of dimethylnitrosamine. *Virchows Arch* 2003, 442:39-47
16. Carthew P. et al., Hepatic fibrosis and iron accumulation due to endotoxin-induced hemorrhage in the gerbils. *J Comp Pathol* 1991, 104:303-311
17. Pietrangelo A. et al., Molecular and cellular aspects of iron-induced hepatic cirrhosis in rodents. *J Clin Invest* 1995, 95:1824-1831

注：本研究は、2002年8月4日【第三回細胞病理談話会(熊本大学医学部)】と2003年2月20日【第二回 Kochi Medical School Research Meeting (高知医大)】で発表した。

作成日：2003年3月10日

**Table 1: Chronological summary of liver injuries, iron deposition and immunohistochemical staining intensity.**

	Necrosis	Fibrosis	Iron	ASMA-positive HSCs in parenchyma	ED-1-positive macrophages	TNF- $\alpha$ -positive macrophages
<b>Normal</b>	-	-	-	-	-	-
<b>Hours 6</b>	-	-	-	-	-	-
<b>12</b>	+	-	-	-	+	+
<b>24</b>	++	-	-	-	+	+
<b>36</b>	+++	-	-	-	+	+
<b>Days 2</b>	+++	-	-	-	++	+
<b>3</b>	+++	-	±	+	++	+
<b>4</b>	++	-	+	++	+++	+++
<b>5</b>	++	-	++	++	+++	+++
<b>7</b>	+	+	+++	+++	+++	+++
<b>10</b>	±	++	+++	++	++	++
<b>14</b>	-	+++	+++	-	++	++
<b>1 Month</b>	-	+++	+++	-	++	+
<b>3 Months</b>	-	+++	+++	-	++	+
<b>6 Months</b>	-	+++	+++	-	++	+

The intensity is graded as: -, negative; +, weak; ++, moderate; +++, high expression.

#### Legends for figures

Fig. 1. Normal rat liver. C: central vein; P: portal tract. HE stain.

Fig. 2. Submassive hemorrhagic necrosis with extension into zones 3 and 2 at 36 hours after DMN injection. C: central vein; P: portal tract. HE stain.

Fig. 3. At day 5 after DMN injection, a large amount of phagocytosing macrophages in the necrotic areas and migration of HSCs into necrotic areas along residual reticular fibers. C: central vein. HE stain.

Fig. 4. At week 1 after injection, thin fibrous septa is formed (arrow). C: central vein. HE stain.

Fig. 5. At week 2 after injection, C-C bridging fibrosis (arrows) is formed. C: central vein; P: portal tract. HE stain.

Fig. 6. At week 2 after injection, Berlin blue staining showed numerous macrophages laden with iron (arrows) in fibrous septa. In inset, high magnification of a macrophage.

Fig. 7. At month 10, a dignificant iron (arrows)deposition is sustained in macrophages in fibrous septa. Berlin blue.

Fig. 8. At week 1 after injection, immunohistochemical staining of  $\alpha$ -smooth muscle actin staining shows activated HSCs (arrows) in necrotic areas and thin fibrous septa.

Fig. 9. ED-1 staining showed plenty of macrophages (arrows) in necrotic area and in fibrous septa.

Fig. 10. TNF- $\alpha$  is expressed in some of the infiltrating macrophages (arrows) in necrotic area and in fibrous septa.

Fig. 11. In in situ hybridization of collagen I at week 2, signals were detected in HSCs (arrows) producing collagen.

Fig. 12. The electron micrograph illustrates one macrophage containing phagocytic debris (M) at days 10 after injection, which is in close proximity to the collagen-producing myofibroblast (My).

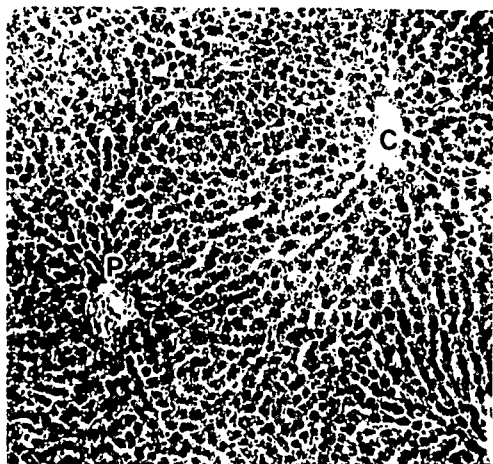


Fig. 1



Fig. 2

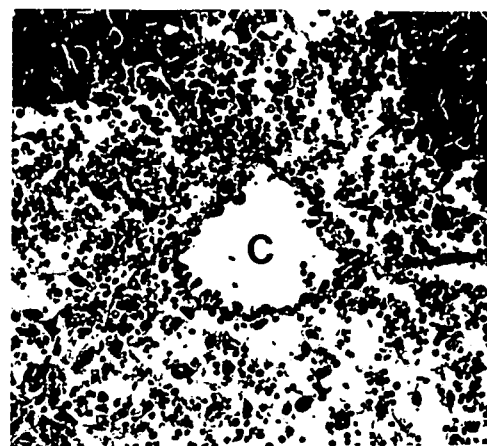


Fig. 3

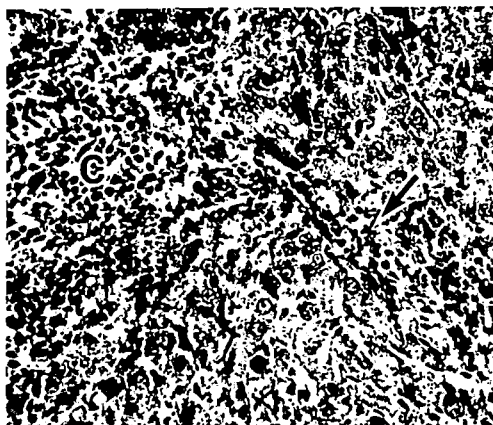


Fig. 4

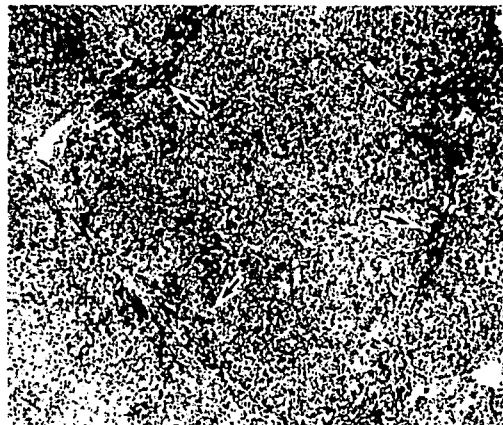


Fig. 5

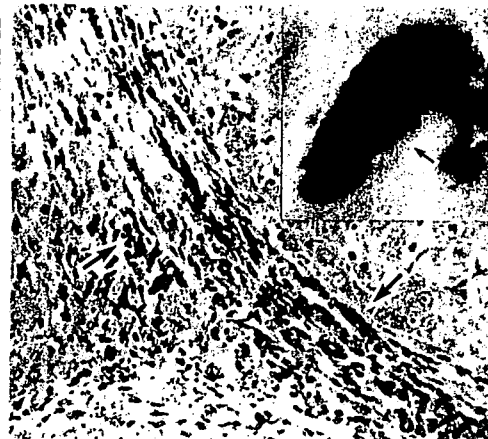


Fig. 6

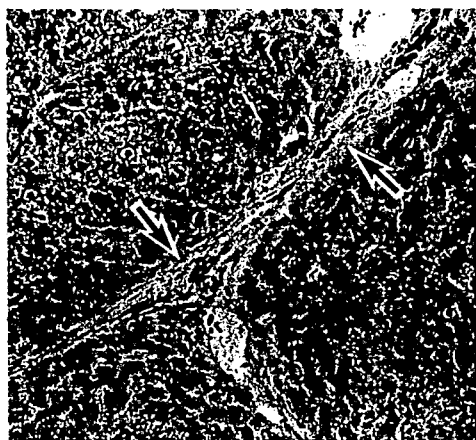


Fig. 7

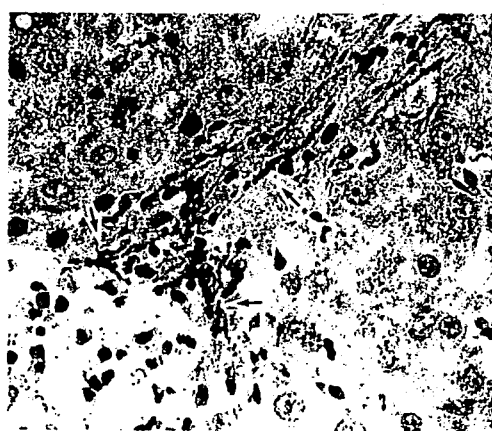


Fig. 8

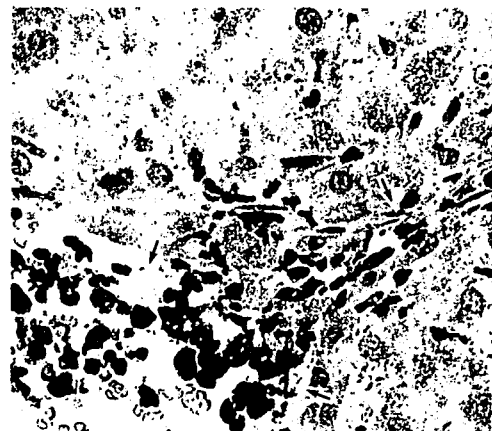


Fig. 9

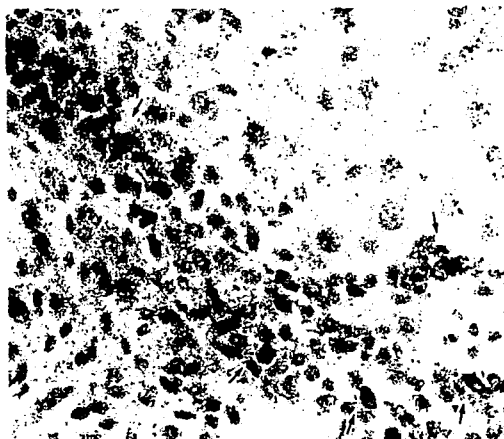


Fig. 10

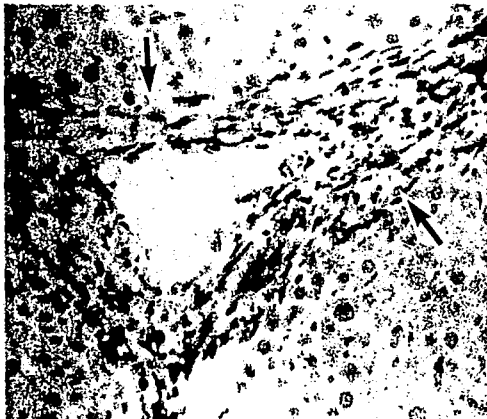


Fig. 11

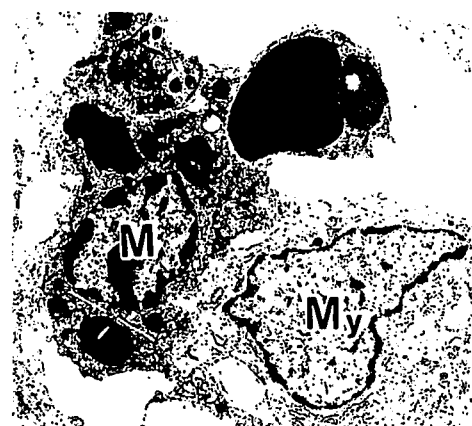


Fig. 12